ELSEVIER

International Journal of Mass Spectrometry 185/186/187 (1999) 837–846

International Journal of Mass Spectrometry

Bimolecular reaction dynamics of $Co^+(^3F_4)$ + acetone reaction in real time

Sung Soo Yi, Emily L. Reichert, James C. Weisshaar*

Department of Chemistry, University of Wisconsin-Madison, Madison, WI 53706-1396, USA

Received 21 July 1998; accepted 29 September 1998

Abstract

A beam of $Co^+(^3F_4)$ is formed at a sharp zero of time by resonant two-photon ionization with a ns dye laser pulse and crossed with a beam of acetone gas under single collision conditions at collision energies $E_t = 0.01$ eV and 0.23 eV. The ion-molecule reaction occurs in field-free space in the extraction region of a time-of-flight mass spectrometer. After a variable time delay $t_{ext} = 0.8 - 8$ μs, a fast high voltage pulse extracts product ions and residual reactant ions into a field-free flight tube for mass analysis. Consistent with earlier work, we observe three product channels, formation of long-lived $CoC_3H_6O^+$ complexes and the two elimination products, $CoCO^+$ (+ C_2H_6) and $CoC_2H_6^+$ (+ CO). The long-lived complexes decay to elimination products and back to Co^+ + acetone reactants on a wide range of time scales, as revealed by retarding field analysis of the metastable decay. Some complexes eliminate C_2H_6 on a 500 ns timescale, as revealed by tailing of the $CoCO^+$ peak. Other complexes still have not decayed on a 25 μs time scale. Deuteration of the acetone substantially decreases the elimination rates. We discuss how angular momentum conservation can lead to nonexponential complex decay and time-dependent product branching. (Int J Mass Spectrom 185/186/187 (1999) 837–846) © 1999 Elsevier Science B.V.

Keywords: Transition metal atom chemistry; Ion-molecule dynamics; Time-of-flight mass spectrometry; Co^+ + acetone

1. Introduction

It is a pleasure to help celebrate Mike Bowers' 60th birthday. As he reaches this major milestone, we congratulate him on his many accomplishments and eagerly anticipate many more productive years to come. One of the very important unifying themes in Mike's work over the years has been the role of angular momentum conservation in ion-molecule reactions. By virtue of the strong long-range attractive forces between an ion and a polarizable neutral, ion-molecule reaction cross sections can of course be very large, as most simply described by the Langevin ion-induced dipole "capture cross section" [1,2] dating to 1905. For example, in $Ni^+ + C_3H_8$ at 0.21 eV collision energy, the Langevin cross section is 90 Å^2. For neutrals that possess a permanent dipole moment, the capture cross section becomes even larger. Su, Chesnavich, and Bowers led early efforts to parametrize these effects with their "average dipole orientation" (ADO) models [3–5], developed in 1973. More sophisticated models have followed [6,7], but these early efforts brought the most important physical effects into sharp focus.

Such capture cross sections imply that bimolecular collisions with large impact parameters and thus large

* Corresponding author.

Dedicated to Professor Michael T. Bowers on the occasion of his 60th birthday.

PII S1387-3806(98)14210-0

orbital angular momenta can reach distances at which chemical bonding becomes important. In the same $Ni^+ + C_3H_8$ example, collisions with l as large as 272 can penetrate the centrifugal barrier at 0.21 eV collision energy. In the relatively recent past, both the ion-molecule community and our friends in the neutral–neutral reaction community [8] have come to appreciate how important the effects of angular momentum conservation can be. Angular momentum can strongly affect the overall reaction cross section or rate constant as well as product branching and their dependence on collision energy, temperature, and pressure.

A wide variety of bimolecular ion-molecule reactants fall into deep potential wells without a barrier to form long-lived collision complexes. Subsequent barriers en route to products can then lead to many intriguing angular momentum effects. For example, the overall reaction efficiency may be much smaller than unity even though the reaction is exothermic and all barriers lie 5–10 kcal/mol *below* the reactant energy. The Bowers group has been active in unraveling these effects in the reactions of transition metal cations M^+ with organic molecules [9–14].

Many groups have been deeply involved in studies of transition metal cation reactions with alkanes and alkenes over the past decade [15–19]. In recent studies of $M^+ +$ alkane reactions, we have developed a new crossed-beam technique based on time-of-flight mass spectrometry that can monitor the decay of long-lived bimolecular complexes *in real time* following initiation of ion-molecule collisions at a sharp zero of time using an ionizing laser pulse [19–21]. In our most complete study to date, we recently reported on the reaction of Ni^+ with C_3H_8 [21], which produces both H_2 and CH_4 elimination products. By comparing experimental data from our group and from the Bowers and Armentrout groups with the results of statistical rate modeling based on electronic structure theory, we were able to construct a rather comprehensive picture of the mechanism of the reaction [22]. Angular momentum conservation and the existence of *tight transition states* slightly below the energy of reactants plays a key role in the product branching. This was first discussed by Bowers, Beauchamp, and Armentrout [12]. Our model indicates that at fixed kinetic energy, only low-J complexes can eliminate H_2 or CH_4; high-J complexes encounter large centrifugal barriers along elimination paths and eventually return to $Ni^+ + C_3H_8$ reactants after a long time delay [22].

Here we present analogous time-resolved experimental results for an another CC bond breaking reaction, $Co^+ +$ acetone. The three product channels observed are [14]:

$$Co^+ + C_3H_6O \longrightarrow \begin{cases} CoC_3H_6O^+ & \text{(1a)} \\ CoC_2H_6^+ + CO \quad -\Delta H = 1.02\ \text{eV} & \text{(1b)} \\ CoCO^+ + C_2H_6 \quad -\Delta H = 1.50\ \text{eV} & \text{(1c)} \end{cases}$$

The new data complement earlier work on the same reaction by the Freiser group [23] who explored the dissociation of products induced by collisions or by multiphoton infrared absorption; by Armentrout, Beauchamp and co-workers [24], who used labeling to infer mechanistic details, and by the ubiquitous Bowers group [14], who studied product kinetic energy release distributions (KERDs). The existence of so much data makes $Co^+ +$ acetone another natural testing ground for electronic structure treatments of the energetics along the entire reaction path.

2. Experimental

2.1. Crossed-beam measurements

The crossed-beam apparatus and its usual operating parameters have been described previously

[21,25]. In the source chamber, gas-phase cobalt atoms are produced in a laser ablation source [26,27] and seeded into an argon beam, which is skimmed and collimated. Electric fields strip ions from the beam. In the interaction chamber, the Co atoms are ionized by a pulsed dye laser, initiating bimolecular ion-molecule collisions. The Co^+ cations react in field-free space with acetone molecules from a second pulsed valve. After a suitable reaction delay, a high voltage pulse extracts reactant and product ions into the time-of-flight mass spectrometer (TOF-MS) for analysis. The experiment runs in the single-collision regime.

A frequency-doubled dye laser (10 ns full width at half maximum (*FWHM*), 312 nm, <250 μJ/pulse) intersects the atomic beam and resonantly photoionizes Co via the $y^4D^\circ_{7/2} \leftarrow a^4F_{9/2}$ transition at 32 028 cm^{-1} [28,29]. Absorption of two such photons creates Co^+ exclusively in the ground spin–orbit level ($^3F_4$). The two-photon energy lies 491 cm^{-1} above the ionization energy of 63 565 cm^{-1} [30]. The nearest Co^+ excited state is $^3F_3$ at 951 cm^{-1} above the IE. A log–log plot of Co^+ ion yield vs laser pulse energy is linear with slope of unity, consistent with a two-photon process whose first step is saturated.

The metal ion velocity is that of the neutral beam, $(5.8 \pm 0.5) \times 10^4$ cm/s [25]. The packet of Co^+ (2000–7000 ions/shot) intersects the beam of acetone in the extraction region of a Wiley-McLaren time-of-flight mass spectrometer [31]. The vapor pressure of acetone above the cooled liquid (60 Torr at −2 °C) [32] is expanded neatly from a second 0.5 mm pulsed nozzle and pseudo-skimmed (i.e. not differentially pumped) by a set of home-built rectangular knife edges. The mean acetone beam velocity measured with a fast ion gauge is $(7.0 \pm 1.0) \times 10^4$ cm/s. We see no evidence of heavier products that might indicate the presence of a significant fraction of dimers in the acetone beam. In addition, plots of product yield vs acetone backing pressure are linear from 20–120 Torr, indicating that single collision conditions are obtained at 60 Torr and further suggesting that the beam consists primarily of monomers. Based on expansions of propane under similar conditions [33], we estimate that the internal temperature of acetone is roughly 50 K.

By changing the angle between the Co^+ and acetone beams, we can vary the collision energy in coarse steps. We have conducted experiments at two such geometries, 20° and 145°. The corresponding collision energies are 0.01 ± 0.01 eV (0.2 ± 0.2 kcal/mol) and 0.23 ± 0.09 eV (5.3 ± 2.1 kcal/mol). The estimated uncertainties reflect worst-case analyses accounting for uncertainties in the metal and acetone velocities, small additional velocity imparted to the metal ions by space charge effects, and the range of angles of intersection of the two velocity vectors.

The 10 ns laser pulse initiates ion-molecule collisions at a sharply defined starting time. After a variable delay time that allows collisions to occur, reactant and product ions are extracted at time t_{ext} after the laser pulse into the TOF-MS for analysis. We can obtain useful signals for extraction times in the range $0.5\ \mu s \leq t_{ext} \leq 8\ \mu s$. At t_{ext}, high voltage pulses (1–1.5 kV) are applied to the ion extraction plates, accelerating reactant and product ions toward the detector. The voltage pulses rise to 90% of their plateau values in 20 ns; the analogous rise time of the electric field in the first extraction region is about 13 ns. The mass resolution ($m/\Delta m$) is >250 for products near 100 u. Ions are detected with a microchannel plate detector (Galileo FTD-2003) operated at 2×10^7 gain. Detector output current drops over the 50-Ω load on a LeCroy 9400 digital oscilloscope without further amplification. We estimate detector mass-discrimination effects at less than 10% [34]. Because the detector dynamic range cannot simultaneously accommodate Co^+ and the much smaller product ion signals, a small set of electrodes mounted in the drift region is pulsed at the appropriate time to deflect Co^+ ions away from the detector [25].

Under single collision conditions, total product signal should rise linearly with Co^+ number density, hydrocarbon number density, and t_{ext}, which we have experimentally verified. Moreover, the reaction should be insensitive to argon backing pressure. We have run the experiment at twice and half the normal argon backing pressure of 1.7 atm with $t_{ext} = 8\ \mu s$

and observe no changes in branching fractions or product yield relative to Co^+ ions.

It is important to distinguish clearly two different time scales. The first is the experimental time window during which the Co^+ and acetone reactant beams are "in contact" and collisions at a well defined energy may occur. This is the time between the ionizing laser pulse and the ion extraction pulse at t_{ext}. The second, which we simply call t, refers to the time since a long-lived complex was formed in a bimolecular collision. Because our experiment is firmly in the single-collision limit, to a good approximation we create collision complexes with a uniform distribution of initiation times over a time window of width t_{ext}. When we sample the fate of this collection of complexes at a particular real experimental time after the ionizing laser pulse, as in a TOF mass spectrum, we sample complexes that have evolved over a corresponding distribution of times t after initiation of the collision. This is range of times referred to in subsequent tables of time-dependent product branching fractions.

2.2. Analysis of metastable decay by retarding potential method

Under our controlled reaction conditions, the product mass spectra reveal long-lived $CoC_3H_6O^+$ collision complexes [Eq. (1a)]. Such complexes have survived extraction intact, because they arrive at the detector at appropriate times for the adduct ion. For the typical ion extraction energy of 1380 eV, the time during which $CoC_3H_6O^+$ is accelerated by the extraction fields is about 2 μs. These complexes are metastable. They have sufficient energy to fragment either to $Co^+ + C_3H_6O$ reactants or to exothermic $CoC_2H_6^+ + CO$ [Eq. (1b)] or $CoCO^+ + C_2H_6$ [Eq. (1c)] elimination products. For $t_{ext} = 8$ μs, complexes that survive $t = 2 - 25$ μs after they are formed may fragment in the field-free drift region of the mass spectrometer. Even longer-lived complexes will reach the detector intact.

Such metastable decay can be analyzed by applying a retarding potential in the flight tube between the reaction zone and the detector, as described previously (Fig. 2 of [21]). The retarding potential device alters arrival times in a mass-dependent fashion by first decelerating and then accelerating the ions back to their original drift velocity. In the examples presented later, we are able to distinguish long-lived $CoC_3H_6O^+$ complexes that survive the entire flight path intact, complexes that fragment in the first field-free region F1 before entering the retarding field, and complexes that fragment in the retarding potential device, region R. Neutral fragments formed in F1 also create a distinguishable peak whose arrival time is insensitive to retarding field voltage V_r.

3. Results

3.1. Co^+ + acetone at $E_t = 0.01$ eV and 0.23 eV

As shown in Fig. 1, at collision energy $E_t = 0.01$ eV with $t_{ext} = 8$ μs the dominant product 81 ± 2% is the long-lived complex $CoC_3H_6O^+$. We also see 16 ± 1% of the C_2H_6 elimination product $CoCO^+$, and 4.0 ± 0.5% of the CO elimination product $CoC_2H_6^+$. At $E_t = 0.23$ eV and $t_{ext} = 8$ μs, we observe the same product ions but with elimination products in higher proportion. The branching fractions are 66 ± 2% $CoC_3H_6O^+$, 28 ± 2% $CoCO^+ + C_2H_6$, and 6.0 ± 0.5% $CoC_2H_6^+ + CO$. The ratio of $CoCO^+$ to $CoC_2H_6^+$ intensity remains relatively constant with collision energy. However, notice that the $CoC_3H_6O^+$ adduct ion peak is broadened at the higher energy. This is because of the metastable decay of the adduct in the drift region of the mass spectrometer prior to striking the detector and slight separation of the parents and fragments in time because of the strong electric field at the detector. The retarding field will separate these fragment and parent ions cleanly in time, as described later.

The simple TOF-MS with $t_{ext} = 8$ μs (Fig. 1) in effect samples the decay kinetics of collision complexes over a uniform distribution of times in the window $t = 2 - 10$ μs because of initiation of a collision, as explained in detail earlier [21]. The resulting "prompt" product branching fractions including adducts are summarized in Tables 1 and 2. In

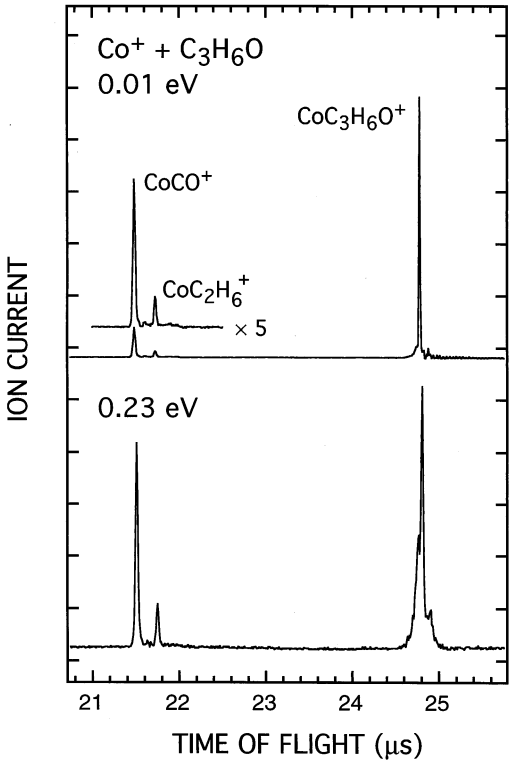

Fig. 1. Time-of-flight mass spectra of product region following collisions of $Co^+ + C_3H_6O$ with ion extraction time $t_{ext} = 8$ μs and collision energy $E_t = 0.01$ eV (top panel) and 0.23 eV (bottom panel).

Tables 3 and 4, we compare the branching between the two elimination products under our conditions with that observed in earlier work [9,23,24]. The branching between C_2H_6 and CO elimination is fairly insensitive to differences in collision energy and perhaps in electronic state distribution of Co^+ among the different experiments.

The ratio of $CoCO^+$ to $CoC_2H_6^+$ intensity is constant, 4.5 ± 0.5, for t_{ext} in the range 2–12 μs. This indicates that C_2H_6 and CO elimination occur on quite similar time scales, as if both channels share a common rate-limiting step. The peaks from the two elimination products are comparably narrow for large extraction times. However, at 0.23 eV with $t_{ext} = 0.8$ μs, the $CoCO^+$ peak clearly exhibits a tail toward longer times (Fig. 2), the characteristic signature of metastable complex decay in the extraction region of the mass spectrometer. The ions in the tail accelerate initially as adduct ions $CoC_3H_6O^+$, fragment during extraction, and complete their acceleration as lighter $CoCO^+$ elimination products. A single exponential decay with 550 ± 100 ns lifetime provides a sensible simultaneous fit of both the narrow component and the tail of the $CoCO^+$ peak. Near 21.6 μs, the tail shows some deviation from that predicted by single exponential decay, as rationalized below. At 0.01 eV,

Table 1
Branching fractions for Co^+ + acetone including complexes, t = 2 − 10 μs after collision[a]

E_t(eV)[b]	$CoCO^+$	$CoC_2H_6^+$	$CoC_3H_6O^+$
0.01	16 ± 1	4.0 ± 0.5	81 ± 2
0.23	28 ± 2	6.0 ± 0.5	66 ± 2

[a] Data for $t_{ext} = 8$ μs and ion extraction energy 1380 eV, which places the time since initiation of Co^+ + acetone in the range 2–10 μs.
[b] Collision energy.

Table 2
Branching fractions for Co^+ + acetone d_6 including complexes, t = 2 − 10 μs after collision[a]

E_t(eV)[b]	$CoCO^+$	$CoC_2D_6^+$	$CoC_3D_6O^+$
0.01	5.5 ± 0.5	0.5 ± 0.2	94 ± 2
0.23	10.4 ± 0.6	1.4 ± 0.3	88 ± 2

[a] Data for $t_{ext} = 8$ μs and ion extraction energy 1380 eV, which places the time since initiation of Co^+ + acetone d_6 in the range 2–10 μs.
[b] Collision energy.

Table 3
Comparison of elimination product branching fractions for Co^+ + acetone

E_t(eV)	Technique[a]	$CoCO^+ + C_2H_6$	$CoC_2H_6^+ +$ CO	Ref.
0.01	CB	82	18	this work
0.23	CB	82	18	this work
TE[b]	ICR	94	6	[23]
~0.5	IB + G	90	10	[24]

[a] CB: crossed beams; ICR: ion cyclotron resonance; IB + G: ion beam plus gas cell.
[b] Thermal energy distributions near 300 K.

Table 4
Comparison of elimination product branching fractions for Co^+ + acetone d_6

E_t(eV)	Technique[a]	$CoCO^+ + C_2D_6$	$CoC_2D_6^+ + CO$	Ref.
0.01	CB	92	8	this work
0.23	CB	88	12	this work
TE[b]	TMS	80	20	9
~0.5	IB + G	90	10	24

[a] CB: crossed beams; IB + G: ion beam plus gas cell; TMS: tandem mass spectrometry.
[b] Thermal energy distributions near 300 K.

the intensity of the $CoCO^+$ peak was too small to observe a clear tail at shorter t_{ext}.

The long-lived $CoC_3H_6O^+$ complexes form the bulk of the products observed in this work. The fraction of these adducts at $t_{ext} = 8$ μs is 66 ± 2% at 0.23 eV and 81 ± 2% at 0.01 eV. This result does not change when the Ar backing pressure is doubled or halved or when the acetone backing pressure varies over the range 20–120 Torr. Formation of Co(acetone)$_2^+$ was not observed. Thus we believe these are bimolecular collision complexes that have *not* been stabilized by a third-body collision.

The metastable decay of these long-lived $CoC_3H_6O^+$ complexes was probed with the retarding potential method. For $t_{ext} = 8$ μs, mass spectra such as those in Fig. 3 in effect sample the decay kinetics of collision complexes over a uniform distribution of times in the window $t = 6 - 24$ μs since initiation of a collision, as explained in detail earlier [21]. For an ion extraction energy of 1380 eV, retarding potentials V_r up to 500 V can separate the $CoC_3H_6O^+$ peak into very long-lived adducts (lifetime > 25 μs) and metastable fragmentation channels, including $Co^+ + C_3H_6O$ and $CoCO^+ + C_2H_6$. At 0.23 eV, 63% of the long-lived complexes fragment after extraction and before exiting the retarding potential device. Of those fragmentation products, 74% are $Co^+ + C_3H_6O$, 24% are $CoCO^+ + C_2H_6$, and less than 2% are

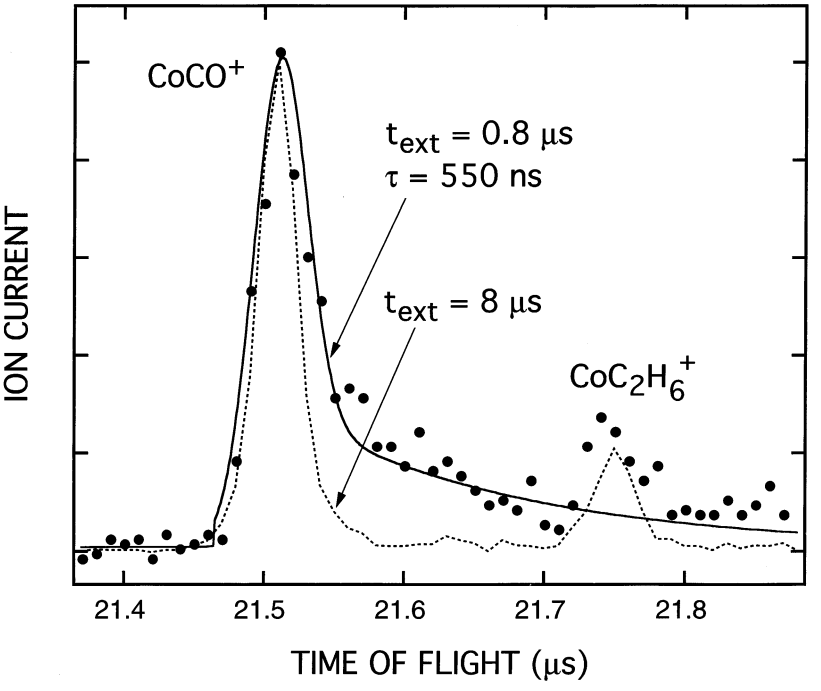

Fig. 2. Expanded view of $CoCO^+$ (+ C_2H_6) peak for $E_t = 0.23$ eV with $t_{ext} = 8$ μs (dotted line) and 0.8 μs (solid dots). For the 0.8 μs data, both the sharp peak and the tail toward longer times can be reasonably fit by a single exponential model of the $CoC_3H_6O^+$ complex decay with $1/e$ time constant of 550 ns, as shown by the solid trace.

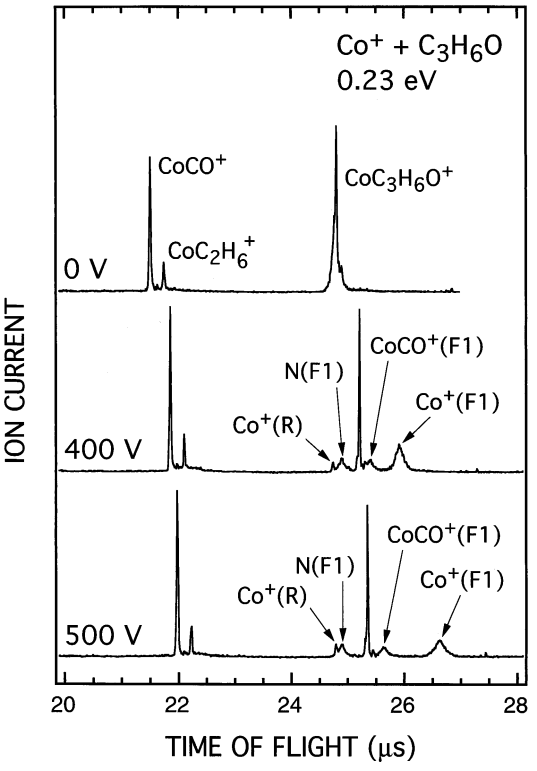

Fig. 3. Retarding field measurements for $Co^+ + C_3H_6O$ at E_t = 0.23 eV and t_{ext} = 8 μs. The broad $CoC_3H_6O^+$ peak in the top trace (retarding voltage V_r = 0) is separated for V_r = 400 V and 500 V into a sharp peak plus fragment peaks as indicated. See text for details.

$CoC_2H_6^+$ + CO. In contrast, at the lower collision energy of 0.01 eV (data not shown), only 18% of the long-lived complexes that survive extraction fragment between the extraction and retarding field regions. Interestingly, at 0.01 eV $CoCO^+ + C_2H_6$ dominates the delayed fragmentation instead of $Co^+ + C_3H_6O$, indicating that the return to reactants has been shut off relative to elimination. These branching fractions from such "delayed" fragmentation are summarized in Tables 5 and 6.

With $V_r \geq 500$ V, all fragments are sufficiently retarded that the $CoC_3H_6O^+$ peak becomes narrow, indicating that a substantial fraction of adduct ions have not yet fragmented when they reach the detector. We measure this quantity most accurately as the ratio of the sharp $CoC_3H_6O^+$ peak to the prompt $CoCO^+$ elimination peak, because both of these peaks should suffer comparably small losses with higher retarding voltages. This ratio is 4.1 ± 0.1 at 0.01 eV and 0.7 ± 0.1 at 0.23 eV.

Table 5
$CoC_3H_6O^+$ fragmentation patterns, t = 6 − 24 μs after collision[a]

E_t(eV)	Fraction dissoc.[b]	Fragment branching		
		Co^+	$CoCO^+$	$CoC_2H_6^+$
0.01	0.18 ± 0.02	33 ± 8	67 ± 8	≤ 2[c]
0.23	0.63 ± 0.13	74 ± 20	24 ± 7	≤ 2[c]

[a] Data for t_{ext} = 8 μs and ion extraction energy 1380 eV. Fragmentation of those ions that survive extraction as adducts but fragment before the retarding field, which places the time since initiation of collision in the range 6–24 μs.
[b] Fraction of complexes that survive extraction region and do not fragment prior to reaching detector.
[c] Upper bound only.

3.2. Co^+ + acetone d_6 at E_t = 0.01 eV and 0.23 eV

For fixed E_t, the average lifetime of Co(acetone)$^+$ adducts increases substantially upon deuteration (Fig. 4). The fraction of adducts in the simple TOF-MS increases to 94% at 0.01 eV and to 88% at 0.23 eV. The prompt product branching fractions (t = 2 − 10 μs) for deuterated acetone with t_{ext} = 8 μs are collected in Table 2. For both acetone and acetone d_6, C_2H_6 elimination is favored over CO elimination by about a factor of 5.

Table 6
$CoC_3D_6O^+$ fragmentation patterns, t = 6 − 24 μs after collision[a]

E_t(eV)	Fraction dissoc.[b]	Fragment branching		
		Co^+	$CoCO^+$	$CoC_2D_6^+$
0.01	0.11 ± 0.02	27 ± 15	73 ± 22	≤ 1[c]
0.23	0.41 ± 0.07	80 ± 18	20 ± 6	≤ 1[c]

[a] Data for t_{ext} = 8 μs and ion extraction energy 1380 eV. Fragmentation of those ions that survive extraction as adducts but fragment before the retarding field, which places the time since initiation of collision in the range 6–24 μs.
[b] Fraction of complexes that survive extraction region and do not fragment prior to reaching detector.
[c] Upper bound only.

For the reaction of Co^+ with acetone d_6, the intensity of the $CoCO^+$ peak was too small to observe a clear tail at shorter t_{ext}. We have recorded retarding-field mass spectra. They are qualitatively similar to the acetone spectra but of lower intensity since far fewer Co(acetone d_6)$^+$ adducts fragment. The resulting branching fractions from delayed fragmentation ($t = 6 - 24$ μs) appear in Table 6. Most of the Co(acetone d_6)$^+$ adduct ions reach the detector without fragmentation, i.e. they survive at least 25 μs. The ratio of the remaining narrow $CoC_3D_6O^+$ peak to the prompt $CoCO^+$ elimination peak for $V_r \geq 500$ V is 13.4 ± 0.4 at 0.01 eV and 3.9 ± 0.1 at 0.23 eV.

4. Discussion

Bowers and co-workers earlier measured kinetic energy release distributions (KERDs) for loss of CO and of C_2D_6 from long-lived $CoC_3D_6O^+$ complexes formed in Co^+ + acetone d_6 bimolecular collisions [14]. They interpreted their results in terms of the mechanism:

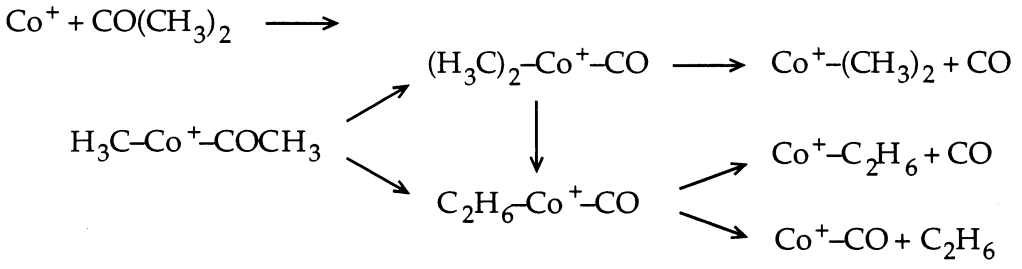

(2)

In particular, both the CO and C_2D_6 KERDs are substantially *colder* than the predictions of phase space theory assuming no substantial barriers along the reaction path. They were able to fit both distributions essentially quantitatively by assuming a common, tight, rate-limiting transition state whose energy lies 9.2 kcal/mol below reactants. The idea is that the centrifugal barrier atop this transition state cuts off reactants with very high angular momentum J. Such high-J collision complexes result from the large range of impact parameters lying within the Langevin capture cross section. In an unrestricted phase space theory, these high-J complexes produce the largest fragment recoil energies, because phase space theory assumes that all centrifugal energy at the exit-channel transition state becomes product translational energy. The same idea can explain why the total reaction cross section, measured earlier by Halle et al. [24], is only 29% of the estimated capture cross section, even though the reaction is highly exothermic [Eqs. (1b) and (1c)]. Based on semiquantitative arguments involving bond energies, Bowers and co-workers suggest that the rate-limiting transition state involves insertion of Co^+ into a CC bond of acetone. The two branches of the reaction scheme of Eq. (2) differ in whether subsequent migration of the second methyl onto the metal center and formation of the $Co^+(C_2H_6)(CO)$ exit-channel complex occurs in two steps or one concerted step.

The most striking feature of our new data is that the elimination reactions occur over a *wide range of time scales*, in spite of good control of reactant electronic, vibrational, and collision energy. In Fig. 2, we see a substantial component of $CoCO^+$ formation on a time scale of about 550 ns (roughly $1/e$ decay time of the complex). In Fig. 3, we see a substantial component of $CoCO^+$ production occuring on a much longer scale of 6–24 μs. In addition, a substantial fraction of the long-lived complexes that survive extraction do not decay at all prior to reaching the detector at $t = 25$ μs. Clearly the decay of even these energetically selected collision complexes is nonexponential.

Metastable decay of long-lived complexes was

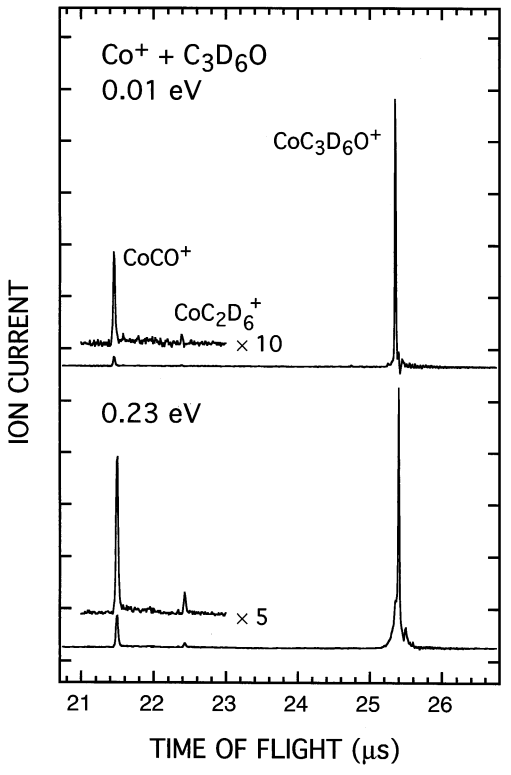

Fig. 4. Time-of-flight mass spectra of product region following collisions of $Co^+ + C_3D_6O$ with ion extraction time $t_{ext} = 8$ μs and collision energy $E_t = 0.01$ eV (top panel) and 0.23 eV (bottom panel).

also observed in the $Ni^+ + C_3H_8$ and $Ni^+ + n-C_4H_{10}$ reactions. The fastest decay component of the long-lived complexes occurs on a sub-200 ns time scale for $Ni(C_3H_8)^+$ formed with $E_t = 0.21$ eV, on a 330 ns time scale for $Ni(C_4H_{10})^+$ with $E_t = 0.21$ eV, and on a 550 ns time scale for $Co(C_3H_6O)^+$ from Co^+ + acetone with $E_t = 0.23$ eV. The decay of the $Co(C_3H_6O)^+$ complexes is slower than either of the $Ni(alkane)^+$ complexes, presumably because the Co^+-acetone potential well is substantially deeper than either Ni^+-alkane well.

We have modeled the $Ni^+ + C_3H_8$ reaction in detail using RRKM statistical rate theory with geometries and vibrational frequencies of stationary points from density functional theory calculations [22]. Theory finds the CC insertion path to be significantly lower in energy than either CH insertion path. The rate modeling indicates that the observed dispersion in complex decay time scales arises from the broad distribution of angular momenta of the complexes, which in turn results from the range of orbital angular momenta contributing to the Langevin cross section. Significantly nonexponential decay occurs when a substantial potential energy barrier restricts the ability of high-J complexes to cross. It is also important that the complex become *more compact in space* on moving from the long-range initial complex $Ni(C_3H_8)^+$ to the rate-limiting transition state. In that case, moments of inertia decrease and the centrifugal effects go in the direction of $k(J)$ decreasing as J increases.

Qualitatively similar effects probably occur for the Co^+ + acetone reaction. Our time-dependent data thus corroborates the "tight transition state" postulated by Bowers and co-workers to explain the statistical KERDs. The suggestion that Co^+ insertion into a CC bond is the rate-limiting step remains sensible. The fact that we observe both CO and C_2H_6 elimination products in constant proportion on all time scales suggests a common "rate limiting step" which may well be CC insertion from the deep complex well. It is perhaps satisfying to suggest that insertion into a CC bond is facile for both acetone and small alkanes, because these are generally the weakest bonds.

However, it is now the task of electronic structure theory to identify the nature of the rate-limiting tight transition state in the Co^+ + acetone reaction. Surprises have occurred in M^+ + alkane reactions, for which density functional theory consistently finds lowest-energy reaction paths involving initial CC insertion and rate-limiting *multicenter transition states.* These transition states are evidently stabilized by strong agostic interactions between CH bonds and the metal cation center. They are not found in calculations of analogous *neutral* M + alkane reaction paths. Surprises could occur in Co^+ + acetone as well.

5. Conclusion

We have reexamined the Co^+ + acetone reaction by preparing reactants in the ground electronic state

with controlled vibrational and translational energy. The time evolution of such carefully prepared long-lived Co^+(acetone) complexes is nonexponential, probably because of the broad range of angular momenta inevitably present in ion-molecule complexes. Our measurements of time-resolved branching fractions stand as an additional critical test of future statistical models. We hope that electronic structure theory will soon be brought to bear on the intriguing question of the nature of the rate-limiting transition state in this reaction.

Acknowledgements

J.C.W. thanks the National Science Foundation and the Donors of the Petroleum Research Foundation for generous support of this research. S.S.Y. acknowledges support from a Lubrizol Fellowship.

References

[1] P. Langevin, Ann. Chim. Phys. 5 (1905) 245.
[2] G. Gioumousis, D.P. Stevenson, J. Chem. Phys. 29 (1958) 294.
[3] T. Su, M.T. Bowers, J. Chem. Phys. 58 (1973) 3027.
[4] T. Su, M.T. Bowers, Int. J. Mass Spectrom. Ion Phys. 17 (1975) 309.
[5] W.J. Chesnavich, M.T. Bowers, Chem. Phys. Lett. 34 (1975) 119.
[6] A.I. Maergoiz, E.E. Nikitin, J. Troe, V.G. Ushakov, J. Chem. Phys. 105 (1996) 6263.
[7] J. Troe, J. Chem. Phys. 105 (1996) 6249.
[8] J. Troe, J. Chem. Soc. Faraday Trans. 90 (1994) 2303.
[9] M.A. Hanratty, J.L. Beauchamp, A.J. Illies, P.A.M. van Koppen, M.T. Bowers, J. Am. Chem. Soc. 110 (1988) 1.
[10] P.A.M. van Koppen, D.B. Jacobson, A. Illies, M.T. Bowers, M. Hanratty, J.L. Beauchamp, J. Am. Chem. Soc. 111 (1989) 1991.
[11] P.A.M. van Koppen, J. Brodbelt-Lustig, M.T. Bowers, D.V. Dearden, J.L. Beauchamp, E.R. Fisher, P.B. Armentrout, J. Am. Chem. Soc. 112 (1990) 5663.
[12] P.A.M. van Koppen, J. Brodbelt-Lustig, M.T. Bowers, D.V. Dearden, J.L. Beauchamp, E.R. Fisher, P.B. Armentrout, J. Am. Chem. Soc. 113 (1991) 2359.
[13] P.A.M. van Koppen, M.T. Bowers, E.R. Fisher, P.B. Armentrout, J. Am. Chem. Soc. 116 (1994) 3780.
[14] C.J. Carpenter, P.A.M. van Koppen, M.T. Bowers, J. Amer. Chem. Soc. 117 (1995) 10976.
[15] K. Eller, H. Schwarz, Chem. Rev. 91 (1991) 1121.
[16] P.B. Armentrout, in Selective Hydrocarbon Activation: Principles and Progress, J.A. Davies, P.L. Watson, A. Greenberg, J.F. Liebman (Eds.), VCH, New York, 1990.
[17] J.L. Beauchamp, P.A.M. van Koppen, in Energetics of Organometallic Species, J.A. Martinho Simoes (Ed.), Kluwer, Dordrecht, 1992.
[18] Organometallic Ion Chemistry, B.S. Freiser (Ed.), Kluwer, Dordrecht, 1996.
[19] J.C. Weisshaar, in State-Selected and State-to-State Ion-Molecule Reaction Dynamics, C.Y. Ng (Ed.), Wiley, New York, 1992.
[20] R.J. Noll, J.C. Weisshaar, J. Am. Chem. Soc. 116 (1994) 10 288.
[21] R.J. Noll, S.S. Yi, J.C. Weisshaar, J. Phys. Chem. 102 (1998) 386.
[22] S.S. Yi, M.R.A. Blomberg, P.E.R. Siegbahn, J.C. Weisshaar, J. Phys. Chem. A 102 (1998) 395–411.
[23] P.I. Surjasasmita, B.S. Freiser, J. Am. Soc. Mass. Spectrom. 4 (1993) 135.
[24] L.F. Halle, W.E. Crowe, P.B. Armentrout, J.L. Beauchamp, Organometallics 3 (1984) 1694.
[25] R.J. Noll, Ph.D. thesis, University of Wisconsin-Madison, 1994.
[26] M.D. Morse, J.B. Hopkins, P.R.R. Langridge-Smith, R.E. Smalley, J. Chem. Phys. 79 (1983) 5316.
[27] D.E. Powers, S.G. Hansen, M.E. Geusic, D.L. Michalopoulos, R.E. Smalley, J. Chem. Phys. 78 (1983) 2866.
[28] J. Sugar, C. Corliss, J. Phys. Chem. Ref. Data 14 (1985) 2 (suppl).
[29] W.L. Wiese, J. Phys. Chem. Ref. Data 17 (1988) 4 (suppl).
[30] R.H. Page, C.S. Gudeman, J. Opt. Soc. Am. B7 (1990) 1761.
[31] W.C. Wiley, I.H. McLaren, Rev. Sci. Instrum. 26 (1955) 1150.
[32] Perry's Chemical Engineers' Handbook, R.H. Perry (Ed.), McGraw-Hill, New York, 1973.
[33] R.J. Gallagher, Ph.D. thesis, Yale University, 1972.
[34] G. Cooper, Y. Zheng, G.R. Burton, C.E. Brion, Rev. Sci. Instrum. 64 (1993) 1140.